small methods
www.small-methods.com

Effects of Processing-Induced Contamination on Organic Electronic Devices

Dimitrios Simatos, Ian E. Jacobs, Illia Dobryden, Małgorzata Nguyen, Achilleas Savva, Deepak Venkateshvaran, Mark Nikolka, Jérôme Charmet, Leszek J. Spalek, Mindaugas Gicevičius, Youcheng Zhang, Guillaume Schweicher, Duncan J. Howe, Sarah Ursel, John Armitage, Ivan B. Dimov, Ulrike Kraft, Weimin Zhang, Maryam Alsufyani, Iain McCulloch, Róisín M. Owens, Per M. Claesson, Tuomas P. J. Knowles, and Henning Sirringhaus**

Organic semiconductors are a family of pi-conjugated compounds used in many applications, such as displays, bioelectronics, and thermoelectrics. However, their susceptibility to processing-induced contamination is not well understood. Here, it is shown that many organic electronic devices reported so far may have been unintentionally contaminated, thus affecting their performance, water uptake, and thin film properties. Nuclear magnetic resonance spectroscopy is used to detect and quantify contaminants originating from the glovebox atmosphere and common laboratory consumables used during device fabrication. Importantly, this in-depth understanding of the sources of contamination allows the establishment of clean fabrication protocols, and the fabrication of organic field effect transistors (OFETs) with improved performance and stability. This study highlights the role of unintentional contaminants in organic electronic devices, and demonstrates that certain stringent processing conditions need to be met to avoid scientific misinterpretation, ensure device reproducibility, and facilitate performance stability. The experimental procedures and conditions used herein are typical of those used by many groups in the field of solution-processed organic semiconductors. Therefore, the insights gained into the effects of contamination are likely to be broadly applicable to studies, not just of OFETs, but also of other devices based on these materials.

1. Introduction

Organic (opto)electronics is a field of research that has enabled the creation of semiconductor devices made from a variety of pi-conjugated compounds, such as conjugated polymers and small molecules. Owing to their mechanical softness and stretchability, low fabrication cost, and their ability to conduct both electrons and ions, organic electronic devices have been used in a broad range of applications, from large-area flexible displays and electronics, to bioelectronics, photovoltaics, and thermoelectrics. Organic electronic devices can be solution-processed and printed, and are often marketed as easy to fabricate and defect-tolerant, in contrast to their inorganic counterparts. While for inorganic semiconductors the severe impact of impurities and process-related contamination on device operation is well appreciated,[1–4] the role of such processing-induced

D. Simatos, I. E. Jacobs, M. Nguyen, D. Venkateshvaran, M. Nikolka, L. J. Spalek, M. Gicevičius, Y. Zhang, S. Ursel, J. Armitage, H. Sirringhaus
Optoelectronics Group
Cavendish Laboratory
University of Cambridge
Cambridge CB3 0HE, UK
E-mail: ij255@cam.ac.uk; hs220@cam.ac.uk

The ORCID identification number(s) for the author(s) of this article can be found under https://doi.org/10.1002/smtd.202300476

DOI: 10.1002/smtd.202300476

D. Simatos, D. J. Howe, T. P. J. Knowles
Yusuf Hamied Department of Chemistry
University of Cambridge
Cambridge CB2 1EW, UK

I. Dobryden
RISE Research Institutes of Sweden
Division of Bioeconomy and Health
Department of Material and Surface Design
RISE Research Institutes of Sweden
11486 Stockholm, Sweden

A. Savva, R. M. Owens
Department of Chemical Engineering and Biotechnology
University of Cambridge
Cambridge CB3 OAS, UK

J. Charmet
School of Engineering—HE-Arc Ingénierie
HES-SO University of Applied Sciences Western Switzerland
2000 Neuchâtel, Switzerland

contamination is generally not well understood in the case of organic semiconductors. Consequently, it is often overlooked in the field, even though its detrimental effects on energy levels,[5] or the performance of devices,[6–10] as well as poor electrical stability linked to fabrication- and storage-induced contamination[11] are well-established.

It is surprising, therefore, that the origins of contamination, or ways to overcome it, have received so little attention. In the field of biology it is well known, for example, that the same disposable plasticware used to fabricate organic electronics can contaminate biological experiments by leaching contaminants that can affect the growth of cell cultures,[12] induce protein aggregation,[13–17] and disrupt biological and biochemical assays.[18–20] Some of the leachables have plasticizing properties,[21] just like solid-state molecular additives used for stabilization,[22–24] which suggests that they can affect a polymer's free volume.[25] Part of the issue is that there are few experimental techniques available to monitor organic contaminants at levels relevant to device operation. As a result, the presence of contaminants during processing and their incorporation into the thin films is rarely monitored. Examples of analytical techniques that are suitable for monitoring contamination in organic thin film processing are mass spectrometry and nuclear magnetic resonance (NMR) spectroscopy. The former technique has been used to detect contaminants in solutions,[18–20] while the latter has been used to detect contaminants in thin organic films.[26,27]

Here we use NMR spectroscopy to detect and quantify contaminants in solutions and thin films. We trace their origin to the glovebox atmosphere and laboratory consumables used during film processing, including disposable needles, plastic pipettes, and plastic syringes. An in-depth understanding of the sources of contamination during organic electronic device fabrication has allowed us to establish clean fabrication protocols and make contamination-free samples with improved performance and stability. We demonstrate how re-introducing small amounts of the identified contaminants as additives, in a controlled manner, can affect the thin-film processing behavior and the electrical properties of organic electronic devices. Our study highlights the role of unintentional contaminants in organic electronic devices and demonstrates that certain stringent processing conditions need to be met to avoid scientific misinterpretation, ensure device reproducibility, and facilitate performance stability. It is important to emphasize that the processing infrastructure and procedures in our nitrogen glovebox, including the laboratory consumables used in the preparation and spin coating of solutions, are typical for experimental conditions used in a wide range of studies in the field of solution-processed organic semiconductors. We, therefore, believe that our findings are relevant to the interpretation of results from a wide range of literature and ongoing studies.

G. Schweicher
Laboratoire de Chimie des Polymères
Faculté des Sciences
Université Libre de Bruxelles (ULB)
1050 Bruxelles, Belgium

I. B. Dimov
Electrical Engineering Division
Department of Engineering
University of Cambridge
Cambridge CB3 0FA, UK

U. Kraft
Department of Molecular Electronics
Max Planck Institute for Polymer Research
55128 Mainz, Germany

W. Zhang, I. McCulloch
Physical Science and Engineering Division
King Abdullah University of Science and Technology (KAUST)
Thuwal 23955-6900, Saudi Arabia

M. Alsufyani, I. McCulloch
Department of Chemistry
University of Oxford
Oxford OX1 3TA, UK

P. M. Claesson
KTH Royal Institute of Technology
School of Engineering Sciences in Chemistry
Biotechnology and Health
Department of Chemistry
Division of Surface and Corrosion Science
10044 Stockholm, Sweden

2. Results and Discussion

Our study was originally motivated by certain irreproducible behavior in the substrate wetting of solutions and the electrical characteristics of organic field-effect transistors (OFETs) fabricated in our inert atmosphere glovebox system with conjugated polymers, such as indacenodithiophene-co-benzothiadiazole (C_{16}-IDTBT), a high-mobility polymer widely studied for OFET applications.[28–31] We also observed contamination-induced effects in several other materials, such as poly(2,5-bis(3-alkylthiophen2-yl)thieno(3,2-b)thiophene) (PBTTT),[32] poly[[2,5-bis(2-octadecyl)−2,3,5,6-tetrahydro-3,6-diketopyrrolo[3,4-c]pyrrole-1,4-diyl]-alt-(2-octylnonyl)−2,1,3-benzotriazole (DPPBTz),[33] poly{[N,N′-bis(2-octyldodecyl)-naphthalene-1,4,5,8-bis(dicaroximide)−2,6-diyl]-alt-5,5′-(2,2′-bithiophene)} (N2200 or P(NDI2OD-T2)),[34] dinaphtho[2,3-b:2′,3′-f]thieno[3,2-b]thiophene (C_8-DNTT),[35,36] and bis(triisopropylsilylethynyl)pentacene (TIPS pentacene).[37] As discussed in detail below, the irreproducibility observed in our IDTBT films could not be explained in terms of any of the controlled process parameters, or the analytical information available on the polymers, such as molecular weight or chemical purity. We suspected processing-induced contamination to be the cause, and decided to undertake a broad and systematic investigation to identify the different sources of contamination and their effects not only on wetting, but also on other thin film processing characteristics, as well as on device performance and stability. Our study revealed that the contaminants can either originate from chemicals present in inert atmosphere gloveboxes used commonly for the fabrication of organic electronic devices, or leach from laboratory consumables (disposable syringes, needles, or pipettes) used during thin film processing.

Figure 1a provides an overview of the various contaminants and contamination pathways from different sources identified in our study, such as the glovebox atmosphere, pipette tips, and syringe needles. Figure 1b illustrates the methodology used in this work to characterize contamination by extracting materials into deuterated chloroform ($CDCl_3$), followed by analysis using solution-state NMR. Solution-state NMR allows us to identify the chemical structure of contaminants and quantify their concentration. Fundamentally, NMR is not a particularly

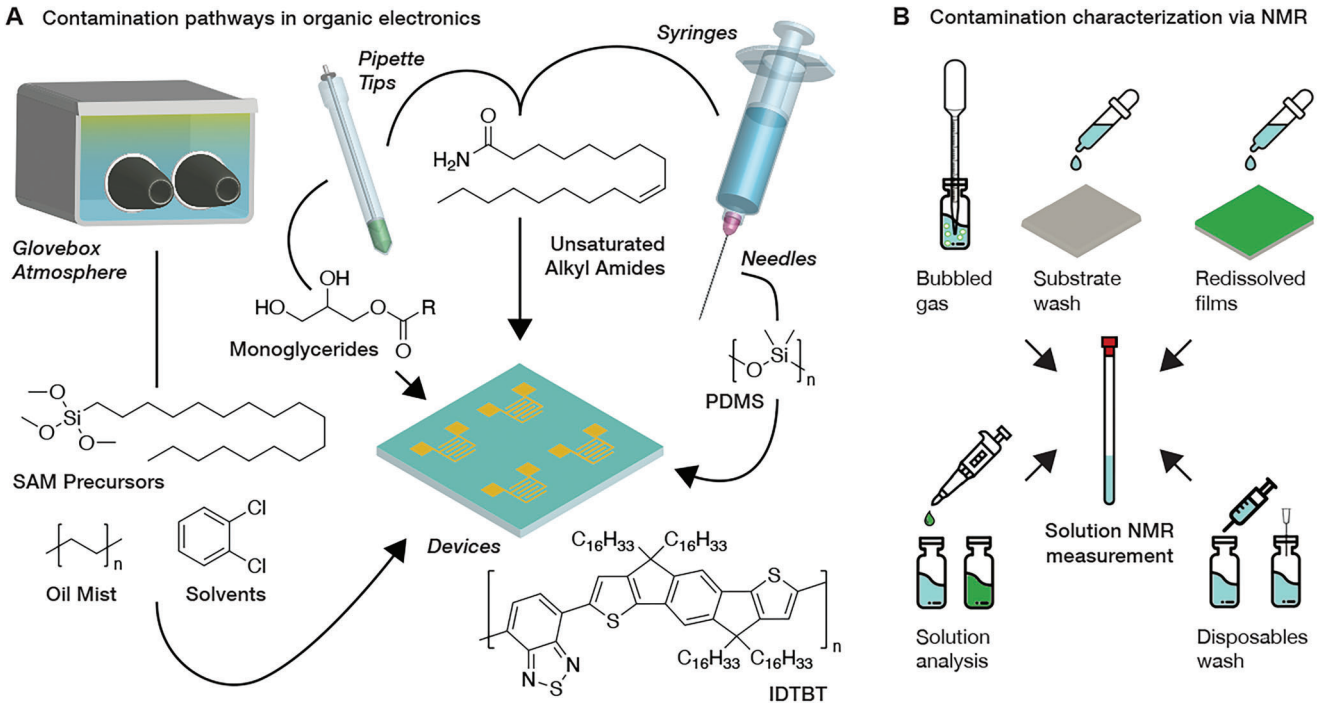

Figure 1. Contamination pathways in organic electronic device fabrication. A) Significant contamination originates from chemicals present in device fabrication gloveboxes, as well as from laboratory consumables commonly used during film processing (syringes, needles, or pipettes). Major contaminants observed from each pathway are shown. B) Contaminants can be identified and quantified via solution-state NMR analysis.

sensitive analytical technique. Even with high magnetic fields of ≈10 Tesla, the Zeeman splitting between nuclear spin levels is only 1% of the thermal energy kT. As a result, the difference in population between spin-up and spin-down states (i.e., the subset of spins that contribute to the NMR signal) is on the order of parts per million. One way to overcome such insensitivity is to redissolve our thin films and measure samples in solution, thereby trading the microstructural information present in solid-state NMR for considerably higher sensitivity. This sensitivity enhancement arises primarily from the extremely narrow linewidths small molecules display in solution, itself resulting from motional averaging caused by molecular tumbling. Recent improvements in the sensitivity of solution-state NMR spectrometers, such as the development of cryoprobes, have enabled the routine detection of nanomole quantities of materials.[38] Such sensitivity is sufficient to detect signals from impurities down to parts-per-thousand (ppt) levels in typical spin coated organic semiconductor thin films.[27]

To characterize the glovebox atmosphere contamination, we used two different NMR experiments, aiming to distinguish between volatile contaminants that exist in the glovebox atmosphere, and nonvolatile ones that condense onto surfaces. To detect volatile contaminants, we analyzed a sample of $CDCl_3$ bubbled with 100 mL of N_2 from the glovebox (depicted as "bubbled gas"). For nonvolatile contaminants condensed onto surfaces, we deposited $CDCl_3$ onto a clean 4 cm × 4 cm glass substrate that had been stored inside the glovebox, then drew the solvent back up and measured its NMR spectrum (labeled "substrate wash"). To detect leachables from laboratory consumables, we washed them with $CDCl_3$ ("disposables wash"). Finally, to detect contaminants in fabricated solutions or thin films, we either mixed 3 µL of solution in 1 mL of $CDCl_3$ ("solution analysis"), or redissolved 4 cm × 4 cm films with $CDCl_3$ ("redissolved films"). The Methods section contains the exact protocols for each one of these NMR methods (Figure S1, Supporting Information). We also recorded a video of the film redissolving process, which is available in the Supplementary Information.

We first focus on the effect of glovebox contamination. In research studies, OFETs are commonly spin coated using halogenated high-boiling point solvents, such as 1,2-dichlorobenzene (DCB).[39] Therefore, we might expect that the main contaminant likely to be found inside a glovebox is residual solvent, generated during spin coating or other solvent-based processes. Residual solvent molecules have been reported to have temporary, stabilizing effects on OFET devices, acting to neutralize moisture-based traps through the formation of solvent-water azeotropes.[24,40] The same solvent-induced stability has been observed when the devices are annealed in a solvent-rich atmosphere,[41] an effect known as "solvent vapor annealing".[42–44] Certain solvents can increase the degree of crystallinity of even weakly crystalline polymers, such as IDTBT, thus improving their bias stress stability.[45] We can use NMR to directly probe the presence of residual solvent in thin films by redissolving them in $CDCl_3$ after any processing steps (e.g., annealing).

Figure 2a shows ^{1}H NMR spectra of redissolved 4 cm × 4 cm thin films of as-cast (blue curve) and 100°C/1 h annealed (orange curve) IDTBT prepared at the outset of our study, before significant steps were taken to reduce glovebox contamination. The green curve (bottom) shows spectra of neat IDTBT for comparison; the peaks at 8.11, 7.95, and 7.40 ppm are the IDTBT

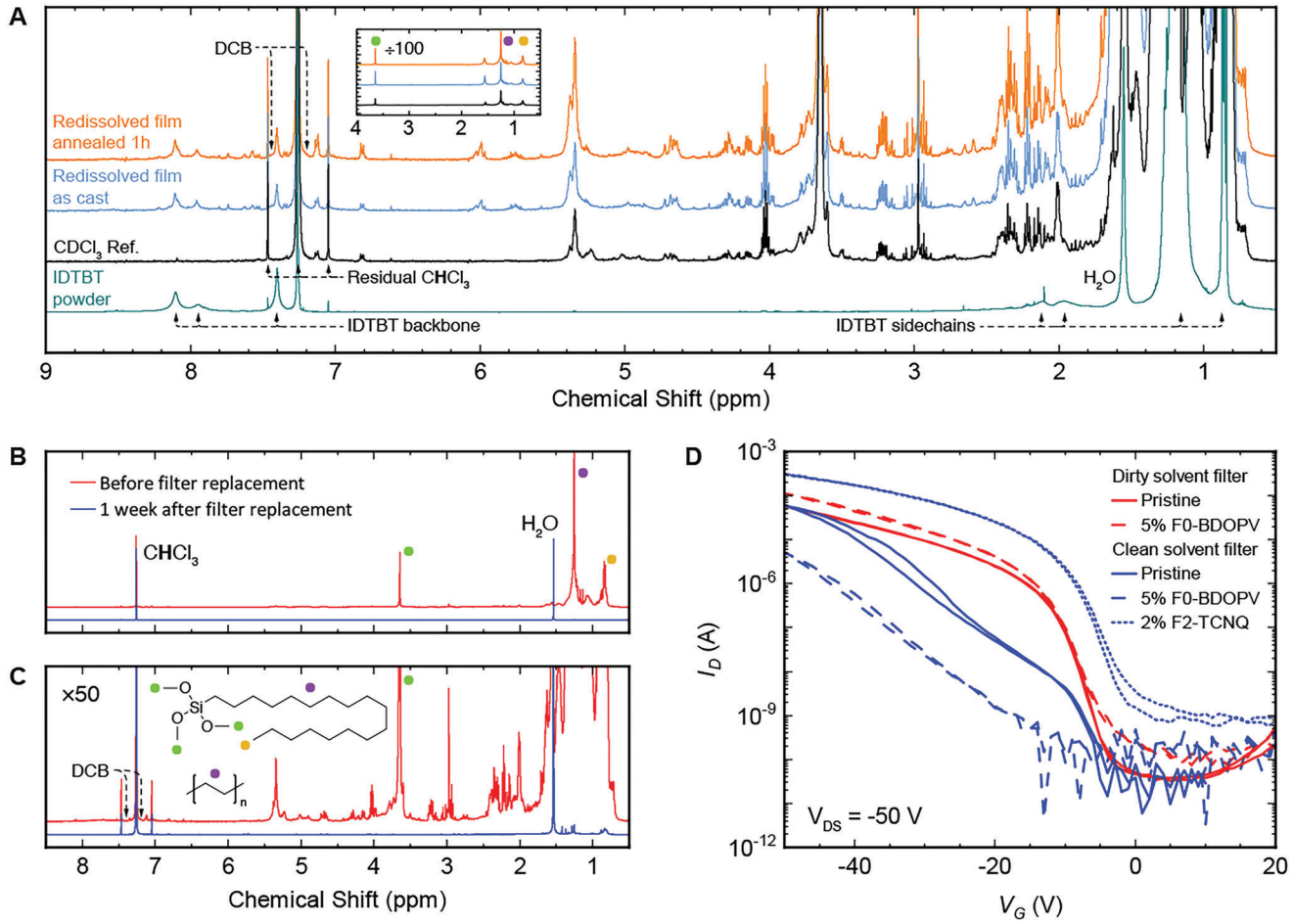

Figure 2. Detection of contamination induced by a saturated solvent filter and its effect on device operation. A) ^{1}H NMR spectra of redissolved 4 cm x 4 cm thin films of as-cast (blue curve) and annealed (orange curves) IDTBT, collected in a contaminated glovebox. The neat IDTBT powder (green curve) is shown for comparison. B) ^{1}H NMR spectra of deuterated chloroform after washing a clean, plasma-treated glass substrate, collected just before solvent filter replacement (red) and 1 week after solvent filter replacement (blue). The three main peaks observed are assigned to alkyltrimethoxysilane self-assembled monolayer (SAM) precursors stored in the glovebox (see structure in (C), inset). C) Detail of (B) scaled by 50*x*, showing a range of other contaminants present in the atmosphere. Expected locations of the most commonly used solvent in the glovebox, DCB, is indicated with arrows. Some impurities present in this spectrum originate from the $CDCl_3$ itself, which had been stored in the glovebox; see the difference spectrum in Figure S2b, Supporting Information. D) IDTBT OFET transfer curves ($V_D = -50$ V) for devices prepared shortly before and shortly after the solvent filter replacement. The NMR and OFET data were taken at different times, ≈12 months apart.

backbone protons, while the peaks below 2.5 ppm correspond to the side chains. The residual protonated solvent peak is visible at 7.26 ppm, along with two ^{13}C satellite peaks, while water appears as a singlet peak at 1.56 ppm. All other peaks visible in the spectra of the redissolved IDTBT films are due to contaminants.

Some of these contaminants are present in the solvent used for the NMR measurements ($CDCl_3$ reference, black curve). Figure S2b, Supporting Information, shows the accumulated contamination in the $CDCl_3$ solvent bottle, with the "3 months" (red) curve being the same dataset as the $CDCl_3$ reference (black) curve in Figure 2a. It can be seen from Figure S2b, Supporting Information that the contaminants contained in the solvent were not visible in earlier measurements from the same solvent bottle, and were therefore introduced during storage or sample processing. In addition, a number of peaks visible in redissolved IDTBT films are not present in the neat IDTBT powder or the $CDCl_3$ used to redissolve the films, and therefore must have been introduced during film processing. Notably, we observe little to no signals from most of the solvents that were used in the glovebox during this period. Only a weak signal from acetonitrile (singlet, 2.10 ppm, used in doping studies of polymer semiconductors) is visible, while n-butyl acetate (triplet, 4.06 ppm, singlet, 2.04 ppm, used to spin coat FET dielectrics), or aromatic solvents such as DCB (doublet of doublets, 7.21 ppm, and 7.45 ppm, used in spin coating) are conspicuously absent. Annealing does not appear to be effective in removing these contaminants. Instead, the annealed sample actually shows slightly higher contamination. As we will discuss in further detail below, this observation suggests that the solvent content in thin films rapidly equilibrates with the solvent atmosphere in the glovebox.

To remove solvent vapor or other volatile materials produced during solution processing, most glovebox systems are equipped with an activated carbon-based solvent filter that can typically absorb ≈500 grams of solvent vapor,[46] provided that the carbon

material is replaced before it becomes saturated. Since there are no volatile organic compound (VOC) sensors that are selective to the commonly used halogenated solvents, there is usually no way to determine when solvent filters become saturated with solvent vapor, or how their filtering efficiency changes as they gradually get filled. As we will demonstrate, the gradual filling of the solvent filter can be monitored by testing the glovebox atmosphere with NMR. The glovebox used for this study was a four-glove MBraun Labmaster 130 glovebox with an activated carbon solvent filter. This is a standard glovebox configuration that is widely used for thin film processing of a wide range of organic and other functional materials. The O_2/H_2O levels always stood at < 1 ppm during the experiments. Despite the application-specific process and equipment used, the general findings of this manuscript can be adapted to other gloveboxes and processes.

Figure 2b shows ^{1}H NMR spectra of $CDCl_3$ after washing a clean, plasma-treated glass substrate ("substrate wash") inside the glovebox. The plasma treatment was performed outside the glovebox. We also performed measurements of the glovebox atmosphere (Figure S2a, Supporting Information) by bubbling 100 mL of glovebox gas through $CDCl_3$ ("bubbled gas"), however, this method proved less sensitive for most contaminants observed in our system (**Figure 3**a). As shown in Figure 2b, before the activated carbon replacement, we were able to detect a range of gas-phase contaminants in our glovebox, although one species was present in considerably higher levels. The dominant species showed only three main ^{1}H signals: a singlet at 3.65 ppm, typical of O–CH_3 groups, as well broader features at 1.25 ppm (CH_2) and 0.85 ppm (CH_3) typical of alkyl chains. Together, these signals are consistent with a trimethoxyalkylsilane such as octadecyltrimethoxysilane (OTMS), one of the self-assembled monolayer (SAM) precursors that were used and stored in the glovebox during this period. This species is also the dominant contaminant observed in redissolved IDTBT films as well (see inset in Figure 2a, inset intensity is divided by 100). However, the integration area of the 1.25 ppm peak is ≈10 times that of the 3.65 ppm peak, while the expected area ratio from the structure of OTMS is ≈3.5. This suggests a secondary aliphatic contaminant is also present. No aliphatic solvents were in regular use during this period, however our NMR analysis reveals that the glovebox vacuum pump oil is a simple aliphatic hydrocarbon and matches well with the 1.25 ppm contamination peak (Figure S26, Supporting Information). We, therefore, suspect that oil mist contamination during antechamber cycling contributes significantly to glovebox atmosphere contamination. Additionally, our NMR data suggests that contaminants from the glovebox atmosphere can find their way into the vacuum pump oil and then be released back into the glovebox, along with the oil mist (Figure S27, Supporting Information). As in the film data, we observe essentially no signal from the most commonly used solvents in the glovebox, such as DCB (arrows indicate expected peak positions in Figure 2c).

After the solvent filter was replaced, essentially all contamination was eliminated within one week. The absence of appreciable residual solvent signals in Figure 2b,c, together with the presence of strong aliphatic signals consistent with SAM precursors and oil mist, leads us to speculate that as the solvent filter begins to saturate, the filtering efficiency for long chain alkanes decreases more quickly than the filtering efficiency for other solvent molecules. This difference in adsorption efficiency likely derives from π–π interactions between solvents and activated carbon: a recent experimental study found that the gas phase adsorption capacity of activated carbon was two orders of magnitude higher for toluene as compared to hexane, an effect attributed to π–π interactions.[47] Furthermore, in toluene-hexane mixtures, the adsorption capacity of hexane dropped further due to competition for adsorption sites. Together these findings suggest that aliphatic compounds, even relatively nonvolatile, long chain materials such as SAM precursors and pump oils, are likely to be the primary contaminants in typical research gloveboxes when the solvent filter is not exchanged regularly.

This accumulation of atmospheric contamination due to declining carbon filtering efficiency can affect the performance of fabricated devices. In particular, it is known from literature that solvents and solid-state additives can improve OFET performance and stability.[24,40,41,45] Similarly, silane-based SAM precursors are highly reactive towards water and can function as p-type dopants[48]; these features could both plausibly lead to stabilization effects in OFETs. We compared OFETs with pristine IDTBT films, i.e., with no intentional addition of solid-state additives, and a Cytop-M dielectric fabricated before and after the activated carbon replacement, to determine the effect of a contaminated glovebox atmosphere on device performance. This study was conducted at a time when contamination was still an issue in our glovebox, i.e., before the implementation of a contamination-free protocol discussed below. The NMR data shown in Figure 2 are representative for the glovebox conditions under which the FETs were fabricated (although the NMR data were obtained at a different time). We also compared pristine OFETs with OFETs that contained 5% w/w benzodifurandione-based oligo(p-phenylenevinylene) (BDOPV or IBDF) and 2% w/w 2,5-difluoro-7,7,8,8-tetracyanoquinodimethane (F2-TCNQ) as solid-state molecular additives. F2-TCNQ has been shown previously to enhance the device performance and operational and environmental stability of IDTBT OFETs in a similar manner as 7,7′,8,8′-Tetracyanoquinodimethane (TCNQ) and 2,3,5,6-Tetrafluoro-7,7,8,8-tetracyanoquinodimethane (F4-TCNQ),[24] while BDOPV is an additive that normally offers no stabilizing benefits.

Pristine OFETs that were fabricated when the solvent trap was near the end of its life, and annealed at 100°C for 1 hour after spin coating, exhibited relatively good device performance with a sharp turn-on and moderately high ON current (Figure 2d). This was somewhat unexpected as we had previously found such pristine and annealed IDTBT OFETs to exhibit poor performance and stability.[24] This suggests that with the solvent trap near the end of its life, performance-enhancing contaminants from the glovebox atmosphere can become unintentionally incorporated into the film. Indeed, after the solvent filter was replaced, pristine devices exhibited a dramatic decrease in device performance and sluggish turn-on characteristics consistent with our earlier study that had been performed with a well-maintained solvent trap.

The glovebox atmosphere also needs to be considered when interpreting the effectiveness of intentionally incorporated molecular additives for improving device performance. When fabricated in a contaminated atmosphere, the incorporation of BDOPV slightly enhances device performance. However, this is an erroneous conclusion: when devices are fabricated in a clean glovebox

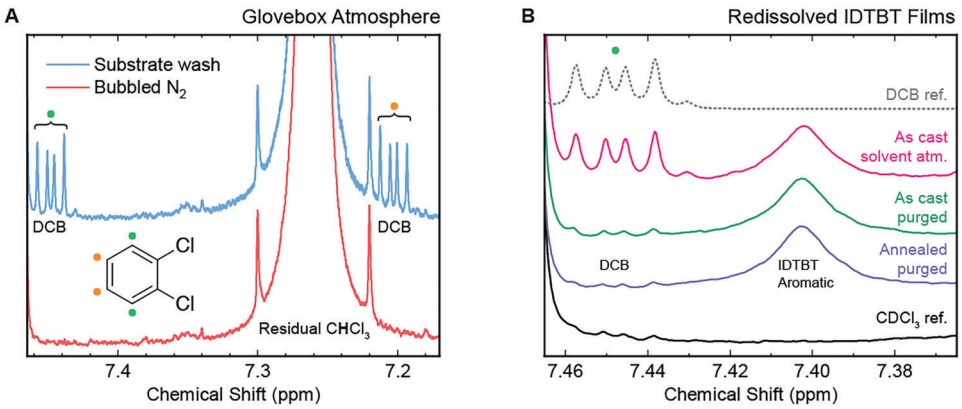

Figure 3. Detection of 1,2-dichlorobenzene (DCB) residual solvent contamination in glovebox atmosphere and thin films. A) ^{1}H NMR spectra of $CDCl_3$ after washing a clean, plasma-treated 4 cm × 4 cm glass substrate (blue curve), or bubbling with 100 mL glovebox gas (red curve). Both NMR samples were fabricated at the same time, shortly after another user had finished spin coating films from DCB. B) ^{1}H NMR spectra of redissolved 4 cm × 4 cm IDTBT films collected in a DCB-rich atmosphere shortly after spin coating (pink curve), in a N_2 purged glovebox after 1 hour of annealing at 100°C (purple curve), or storage at room temperature (green curve).

atmosphere, it becomes clear that BDOPV is in fact not an effective molecular additive (Figure 2d). In contrast, F2-TCNQ is a genuinely effective molecular additive that is able to stabilize devices even in a clean atmosphere, and yield an optimum ON-current. We conclude that it is crucial to maintain a clean glovebox atmosphere when studying the stabilization effects of solid-state additives, to decouple the effects of intentional and unintentional additives, and avoid experimental artefacts. For this reason, we recommend that reported device data should always be accompanied by detailed fabrication protocols, including at a minimum a discussion of the type of solvent trap used in the glovebox, its replacement/regeneration schedule, and details about purging conditions before/during sample preparation.

Based upon the results shown in Figure 2, we upgraded our sample fabrication glovebox with a regenerable molecular-sieve-based solvent trap, and implemented rigorous protocols on solvent use and purging to ensure a clean glovebox atmosphere (see Supporting Information, Experimental Methods Section). Under these conditions, residual solvent from spin coating then becomes indeed the dominant contaminant introduced from the glovebox atmosphere. Figure 3a shows two NMR measurements of the glovebox atmosphere, using the substrate washing and bubbled gas methods, which were fabricated at the same time, shortly after another user had finished spin coating films from DCB. The substrate washing test is able to detect DCB, demonstrating that NMR can be used to test the cleanliness of the glovebox atmosphere and that residual solvents adsorb readily on surfaces in the glovebox. Surprisingly, the bubbled gas test did not detect the DCB, suggesting that for high boiling point solvents such as DCB, aerosols formed during spin coating, rather than direct vapor phase mass transport, may be the dominant contamination pathway.

Figure 3b shows ^{1}H NMR spectra of redissolved 4 cm × 4 cm thin films of IDTBT prepared in a DCB-rich atmosphere shortly after spin coating (pink curve), and films prepared in a N_2 purged glovebox and then annealed for 1 hour at 100°C (purple curve), or storage at room temperature (green curve). The as-cast film prepared in a solvent-rich atmosphere contains significantly more residual DCB compared to both the as-cast and the annealed films prepared in a purged glovebox. The DCB signals in the latter two films are similar in intensity to that of the $CDCl_3$ reference spectrum, so these DCB signals are most likely dominated by solvent adsorbed onto the pipettes or NMR tubes during sample preparation. It is therefore not possible to quantify the exact DCB concentration in these samples. Nonetheless, it is clear that the solvent content in the glovebox atmosphere has a much larger effect on the film's residual solvent content than the annealing conditions.

Together, these results suggest that relatively nonvolatile solvents such as DCB can lead to contamination by adsorbing onto surfaces such as substrates or pipettes. This solvent contamination, both on surfaces and within thin films, should be largely in equilibrium with the solvent vapor in the glovebox atmosphere. In this sense, purging the glovebox reduces most contamination both in films and on surfaces. Annealing is presumably only required to remove the small fraction of kinetically trapped solvent that is not in equilibrium with the atmosphere, and would only be expected to be beneficial when the glovebox atmosphere is completely solvent-free.

Having established the critical role of impurities on device performance, we set out to identify other possible routes of contamination in our devices. In biology, disposable plastic labware, including micropipette tips widely used for preparing solutions and spin coating films, have been reported to leach a wide variety of compounds into aqueous and organic solutions, which can affect the growth of cell cultures,[12] induce protein aggregation,[13–16] and disrupt biological and biochemical assays.[18–20] Oleamide, a lubricant and plasticizing agent commonly used in polypropylene manufacturing, is the most common leachable reported, although a wide range of compounds have been identified by mass spectroscopy and NMR.[18–20] As shown in Figure S3, Supporting Information, our 2D NMR analysis of deuterated chloroform exposed to pipettes is consistent with oleamide being the main leachable, although we also identified an additional leachable: a monoglyceride (likely 1-glycerol monostearate), that was present at about ¼ the concentration of oleamide (Figure S4, Supporting

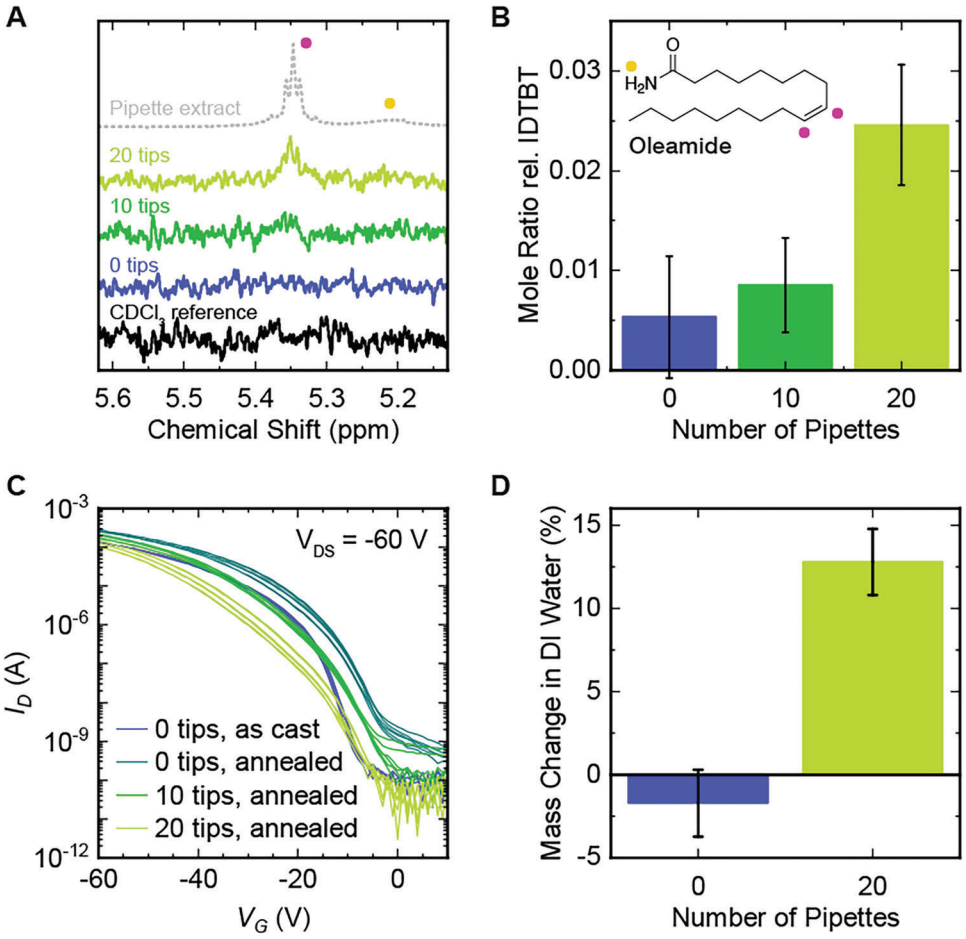

Figure 4. Quantification of oleamide contamination from plastic pipettes and effect on OFET performance. A) ^{1}H NMR spectra of an IDTBT solution after accumulated contamination from plastic pipette tips. Spectra show the unsaturated protons of oleamide at 5.35 ppm (see structure in (B), inset); intensities are normalized to the IDTBT aromatic signal. B) Molar ratio of oleamide to IDTBT monomers in each solution, as determined from the ratio of the integration areas. C) OFET transfer characteristics for devices processed from the solutions shown in (A). D) Quartz crystal microbalance (QCM) measurement of IDTBT film mass increase upon exposure to DI water. Samples were coated with a 100 nm thick Cytop layer to prevent the dissolution of oleamide.

Information). While the amount of contamination from pipettes is relatively small, we observed strong contamination from plastic syringes used in our lab that was consistent with a different unsaturated alkyl amide, along with several additional unidentified species. As shown in Figure S5, Supporting Information, the proton spectra of deuterated chloroform exposed to plastic pipettes and plastic syringes look similar, with only minor differences between the observed functional groups, indicating that the main contaminant leaching from plastic syringes is similar to oleamide but that there are also additional contaminants present.

Although plastic syringes can easily be avoided, micropipettes are vital tools required for repeatable fabrication of organic electronic films to dispense precise amounts of solution as part of a reproducible fabrication process, as well as to minimize waste of small quantities of research organic semiconductor materials. As we have seen above, additives can strongly affect OFET device performance even at the percent level, therefore even a dilute amount of contamination leaching from pipettes could have a significant impact on device performance. Furthermore, a single spin coating solution is often reused for many experiments, and therefore may be exposed to dozens of pipette tips before it is finished. To quantify the effect of accumulated oleamide contamination, we spin coated IDTBT from a freshly prepared solution, and from the same solution after washing with 10 and 20 pipette tips. Each pipette tip was only washed once in the solution. Two sets of films were prepared for each condition—one was used to prepare an OFET, while the other was redissolved and analyzed by NMR. We also collected a sample of each solution before spin coating for NMR analysis. This study was done in a contaminant-free glovebox atmosphere, according to the process described in the Experimental Methods section.

Figure 4a shows ^{1}H NMR spectra of each IDTBT solution, showing the oleamide unsaturated proton signal, along with reference spectra of clean $CDCl_3$ (black line), and $CDCl_3$ washed with 15 pipette tips (gray dotted line). While the reference sample was made by washing pipette tips in $CDCl_3$, the 10 and 20 pipette tips samples were made by washing pipettes in the IDTBT solution, and mixing 5 µL of that solution with 600 µL of $CDCl_3$. All IDTBT solution spectra are normalized to the IDTBT aromatic peaks. The clean spin coating solution ("0 tips") does

not show statistically significant oleamide contamination; only the solutions exposed to pipette tips show visible contamination. Figure 4b shows the molar ratio of oleamide to IDTBT monomers in each IDTBT solution obtained by integrating the IDTBT and oleamide signals. The corresponding ratios for redissolved films are shown in Figure S7c, Supporting Information. We observe somewhat higher contamination in films relative to solutions, perhaps due to aerosolization during spin coating, and condensation onto the pipettes and/or NMR tubes that were used for film redissolution. Precise quantification is difficult due to the low amount of oleamide contamination present–even in the 20 pipette tip solution, we observe only ≈2.5 mol% relative to IDTBT, equivalent to ≈5 ppt oleamide by mass.

Despite the small magnitude of contamination observed in NMR, we still observe a clear, systematic effect of oleamide leachable on OFET device performance. Figure 4c shows transfer curves for IDTBT OFETs prepared from the solutions measured in Figure 4a. We observe a progressive reduction in ON current and more gradual turn-on characteristics with increasing exposure to pipettes, suggesting that oleamide contamination leads to trap formation in IDTBT films. This also leads to a less ideal gate voltage dependence of the mobility (Figure S7e, Supporting Information) and a reduced OFF-state bias stress operational stability (Figure S8, Supporting Information). We plot transfer curves from several devices from each sample in Figure 4c to highlight that device-to-device variation within each processing condition is small.

It is worth noting that, in contrast to Figure 2d, pristine annealed devices fabricated in a clean glovebox now perform well. Additionally, in films coated from oleamide-free solutions, we observe lower performance in nonannealed devices as compared to annealed devices. This behavior is qualitatively different from past reports.[24] We speculate that at least some of the device nonidealities in pristine annealed devices, seen in Figure 2d and our earlier reports, which were fabricated before we had identified leachates as a concern, may originate from oleamide impurities introduced by pipettes and/or syringes. However, some of these performance differences originate from contamination that is intrinsic to the polymer powder. We observe performance variations in cleanly fabricated OFETs made with different IDTBT batches (Figure S9, Supporting Information). We also observe differences in contamination/impurity levels in neat powders of different IDTBT batches (Figure S10, Supporting Information), including the same monoglyceride identified from our pipette leachate spectra. The concentration of this impurity is on the order of 1 mol% in several batches, i.e., the same range where oleamide impurities cause significant changes in device performance. Batches showing these impurities generally show lower device performance in pristine devices (see Table S1, Supporting Information), therefore we suspect that these impurities degrade device performance.

Both oleamide and 1-glycerol monostearate (or similar primary alkyl amides and monoglycerides) should function as surfactants due to their polar head groups and long-chain nonpolar tail. In thin films, we might expect these molecules to aggregate into inverse micelles, forming an emulsion containing hydrophilic voids that are able to attract and hold water more readily than the pristine polymer. To explore this possibility, we used a quartz crystal microbalance (QCM) to precisely measure the mass change of clean and 20-tip contaminated IDTBT films upon exposure to water. Oleamide is slightly water soluble, as confirmed by Fourier-transform infrared (FTIR) measurements of contaminated films after exposure to water (Figure S11, Supporting Information). We therefore coated the QCM samples with a thin (100 nm) layer of Cytop to prevent large water-soluble contaminants (such as oleamide) from leaving the underlying IDTBT film, while allowing water molecules to slowly diffuse through. We note that this structure (substrate/polymer/Cytop) matches that of a top-gate OFET device.

Figure 4d shows the results of this QCM measurement. In the film without pipette tip contamination, we observe no water uptake to within the estimated uncertainty of the measurement. However, in the film contaminated with 20 pipette tips, we see a 12.8% increase in film mass after exposure to deionized (DI) water. This increase in water uptake in contaminated films could conceivably explain the reduction in device performance for contaminated films, consistent with previous evidence that water leads to trap formation in FETs.[24,49] Our QCM data therefore suggest an indirect degradation mechanism, whereby the presence of these emulsifying impurities, introduced both during device processing but also potentially during polymer synthesis, leads to water uptake, which consequently degrades device performance and bias stress stability.

The effects of pipette contamination are not confined to IDTBT, but are also observed in other organic semiconductors. **Figure 5**a–d shows transfer characteristics for DPPBTz, a polycrystalline donor-acceptor polymer, C_8-DNTT, a p-type small molecule semiconductor, N2200, a high mobility n-type polymer, and C_{14}-PBTTT, a highly crystalline p-type polymer. In the first three materials (Figure 5a–c) we observe degraded performance upon contamination, similar to IDTBT (Figure 4c). However, in PBTTT we observe relatively little change in mobility, but rather a very large threshold voltage shift (Figure 5d), along with a large increase in OFF-state bias stress instability (Figure 5e; bias stress data for other polymers are shown in Figures S8 and S14, Supporting Information). We speculate that this OFF-state bias stress instability may also derive from water uptake: protons generated by dissociated water may be able to either directly protonate the organic semiconductor, or accept an electron from band edge states filled during positive gating.[49,50] This effect could, therefore, vary significantly between polymers, depending on the pH of the film, the presence of proton acceptor sites, and the energy level of the band edge.

In addition, we also studied the effect of pipette contamination on sequential doping solutions, commonly used to prepare conducting films for thermoelectric applications. Figure 5f shows the conductivity of PBTTT films coated from a contaminant-free solution, then sequentially doped with an acetonitrile ion-exchange doping solution[51] (100 mM BMP-TFSI / 1 mM $FeCl_3$) that was progressively contaminated with plastic pipettes. We observe a clear reduction in achievable conductivity with increased contamination levels. Therefore, contaminants must also be affecting the redox potential of the dopant solution, indicating that they are redox active within the electrochemical window relevant to organic semiconductor devices. The overall effect of emulsifying, hydrophilic impurities such as oleamide or monoglycerides, therefore, is likely to be incredibly complex, consistent with the range of effects seen in the transfer curves in Figure 5.

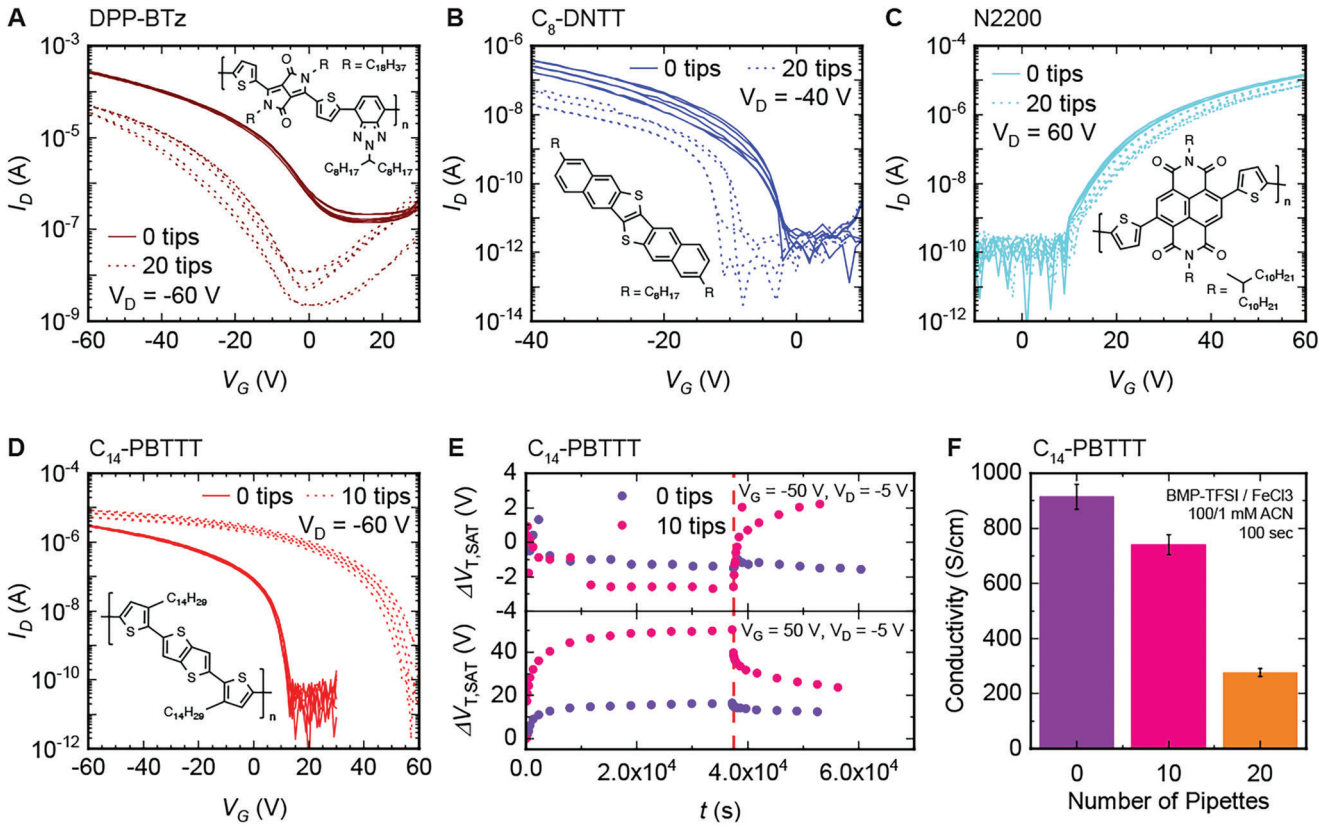

Figure 5. The effect of oleamide leaching from plastic pipette tips on the performance of polymer and small molecule OFETs. The figure shows transfer curves in saturation from A) DPPBTz, B) C_8-DNTT, C) N2200, and D) C_{14}-PBTTT OFETs. Continuous lines denote clean FETs; dotted lines denote contaminated FETs (via pipette washing). E) ON-state and OFF-state bias stress stability of PBTTT OFETs. The vertical line separates the stress and recovery regimes. F) Conductivity of ion-exchange doped PBTTT films.

Other plastic labware can also have a detrimental effect on the performance of polymer OFETs. We observed that filtering a solution of the n-type polymer N2200 using a disposable syringe filter and plastic syringe results in n-type OFETs with larger positive V_T shifts (Figure S15, Supporting Information). Although filtering may alter solution properties in other ways, for example by filtering out high molecular weight or aggregate species, it appears likely that contamination induced by the syringe and/or filter is an important factor contributing to the observed device degradation. Interestingly, plastic contaminant-free N2200 OFETs did not require post-fabrication annealing steps commonly used to improve performance[52] (Figure S16, Supporting Information).

This is not the only effect that plastic leachables can have. High levels of contamination can directly affect the morphology of IDTBT films, with the phase-separated contaminants migrating to the surface of the film (Figure S17, Supporting Information). Pipette contamination was also found to affect the wetting and crystallization behavior of thin films of molecular semiconductors, such as TIPS-pentacene. Pristine solutions of 5 g L^{-1} TIPS-pentacene in DCB were found to dewet easily during typical spin coating conditions with speeds of 1000 rpm. Intentionally contaminating the solution by washing plastic syringes changed its surface tension, enabled wetting, and facilitated the growth of the typically observed spherulite crystal structures (Figure S18, Supporting Information). Oleamide contamination also affected the wetting properties of solution-sheared C_8-DNTT, with the contaminated solution dewetting and the clean solution wetting the substrate (Figure S19, Supporting Information). Finally, contamination affects the solubility of solid-state additives. Contaminated solid-state additive solutions aggregated at room temperature, whereas clean solutions did not (Figure S20, Supporting Information).

We now turn our focus on the effect of contamination on the wetting behavior of polymer films during spin coating, which was the original motivation of this study. When the glovebox atmosphere was still contaminated, we observed evidence that older batches of IDTBT reproducibly yielded uniform, continuous films during spin coating, while more recent polymer batches tended to dewet under nominally identical spin coating conditions. All IDTBT batches had C_{16} side chains and were synthesized by the same chemist, and the difference in wetting properties could not be attributed to differences in synthetic procedures or molecular weight (Table S1, Supporting Information). We suspected that some source of contamination had entered the older batches. There is direct evidence from NMR of the different polymer batches (Figure S10, Supporting Information) for such contamination, however, it has been difficult to trace the source of this contamination as the older batches had been stored in the glovebox and used for several years. However, after eliminating the contamination sources in the glovebox atmosphere and the

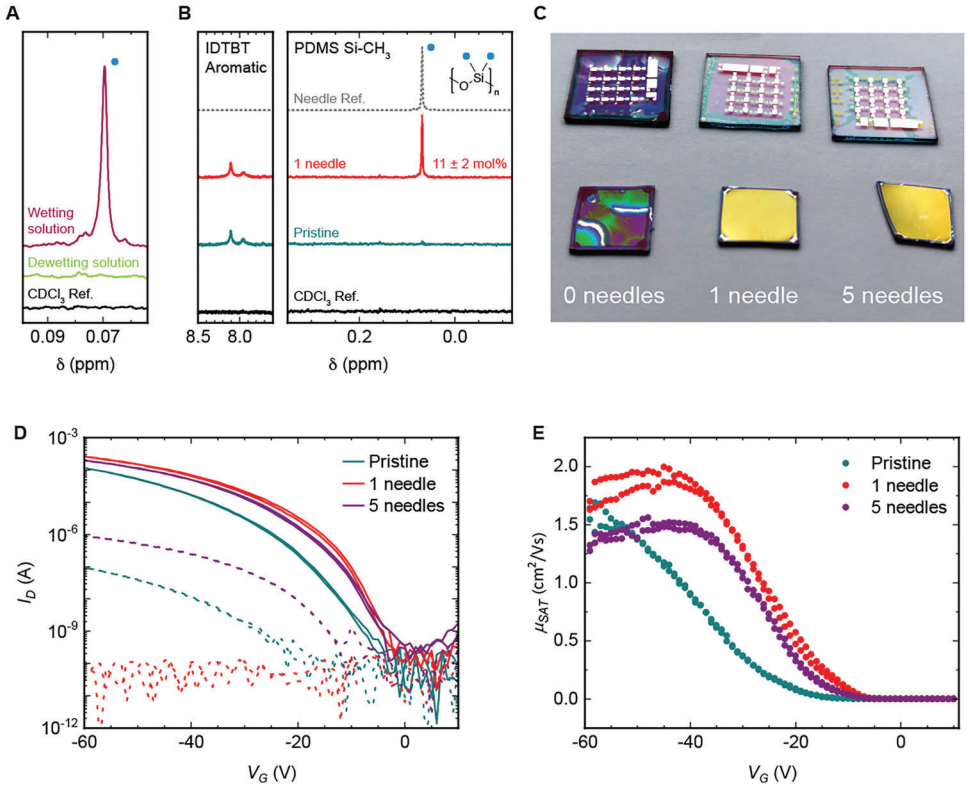

Figure 6. The effect of PDMS on the wetting behavior of IDTBT films, and on device characteristics of IDTBT Cytop-M OFETs. A) ^{1}H NMR of wetting and dewetting solutions. B) ^{1}H NMR of redissolved IDTBT films, showing that syringe needles introduce significant PDMS contamination, matching that seen in wetting solutions. Structure of PDMS is shown in inset. C) Photo of films coated from clean and PDMS-contaminated solutions. Clean IDTBT films consistently dewet from glass and Si substrates, but the introduction of PDMS by dipping one or five needles in the IDTBT solution prior to spin coating leads to good wetting behavior. D) Transfer curves and E) the extracted mobility curves in saturation ($V_D = -60$ V) for three IDTBT OFETs with varying amounts of PDMS contamination. Continuous lines denote the drain current; dotted lines denote the gate leakage current.

oleamide contamination, we observed that there were still experimental runs when, under nominally identical solution preparation and spin coating conditions, solutions of the more recent IDTBT batches were able to wet the substrate and yield perfectly uniform films. We observed that the wetting properties were dependent solely on the polymer solution: solutions that would wet, or dewet, would do so consistently when processed on different days. This suggested another source of processing-induced contamination as yet unidentified.

In order to identify this contamination source, we collected NMR spectra of the wetting and dewetting IDTBT solutions, as shown in **Figure 6**a. The spectra are mostly identical (Figure S21, Supporting Information), except the spectrum of the wetting solution contains a contaminant characterized by a singlet peak at 0.07 ppm, characteristic of Si–CH_3 groups.[53] The source of this contaminant was traced to disposable steel needles used to decant solvents through septum caps. Figure 6b shows a ^{1}H NMR spectrum of $CDCl_3$ into which a needle was dipped, revealing the same singlet signal at 0.07 ppm. No other contamination signals were observed, indicating that all protons in this contaminant are equivalent, and that only a single species leaches from these needles. From this, we can readily identify the contaminant as polydimethylsiloxane (PDMS), a hydrophobic polymer widely used to lubricate medical-purpose syringes and needles (a process known as "siliconization").[54] Recent studies have shown that PDMS can leach into pharmaceutical products,[15,16,55] resulting in what is termed as "Silicone-Oil-Based Subvisible Particles" (SbVPs).[56] In biological research, these leaching PDMS particles have been shown to induce protein aggregation,[13–17] and elicit immunogenic responses.[57] PDMS is hydrophobic,[58] and has plasticizing properties.[59] It could thus conceivably change the wetting, mechanical, and thermal properties of the organic semiconductor,[60] as well as its free volume.[25] Additionally, when plasticizers are incorporated into an amorphous phase, they can lower its glass transition temperature,[61–63] with the latter being linked to the photophysical and charge transport properties of organic semiconductors.[64]

Briefly dipping a needle into an IDTBT solution, and swirling it around for 6–7 s, was enough to contaminate the solution and change its wetting behavior. Figure 6b shows NMR spectra of redissolved IDTBT films coated from a clean solution and a solution that had a needle briefly dipped into it (1 needle / 200 µL solution). We observe significant PDMS contamination in the needle-dipped film: integrating PDMS and IDTBT signals indicates the film is 11 ± 2 mol% PDMS, equivalent to 0.63% by mass. The change in wetting properties is readily apparent in photos of the films shown in Figure 6c. We also recorded a video of the spin coating process with clean and contaminated solutions, which is available in the Supplementary Information. It is worth noting that contamination from plastic pipettes can also modify the

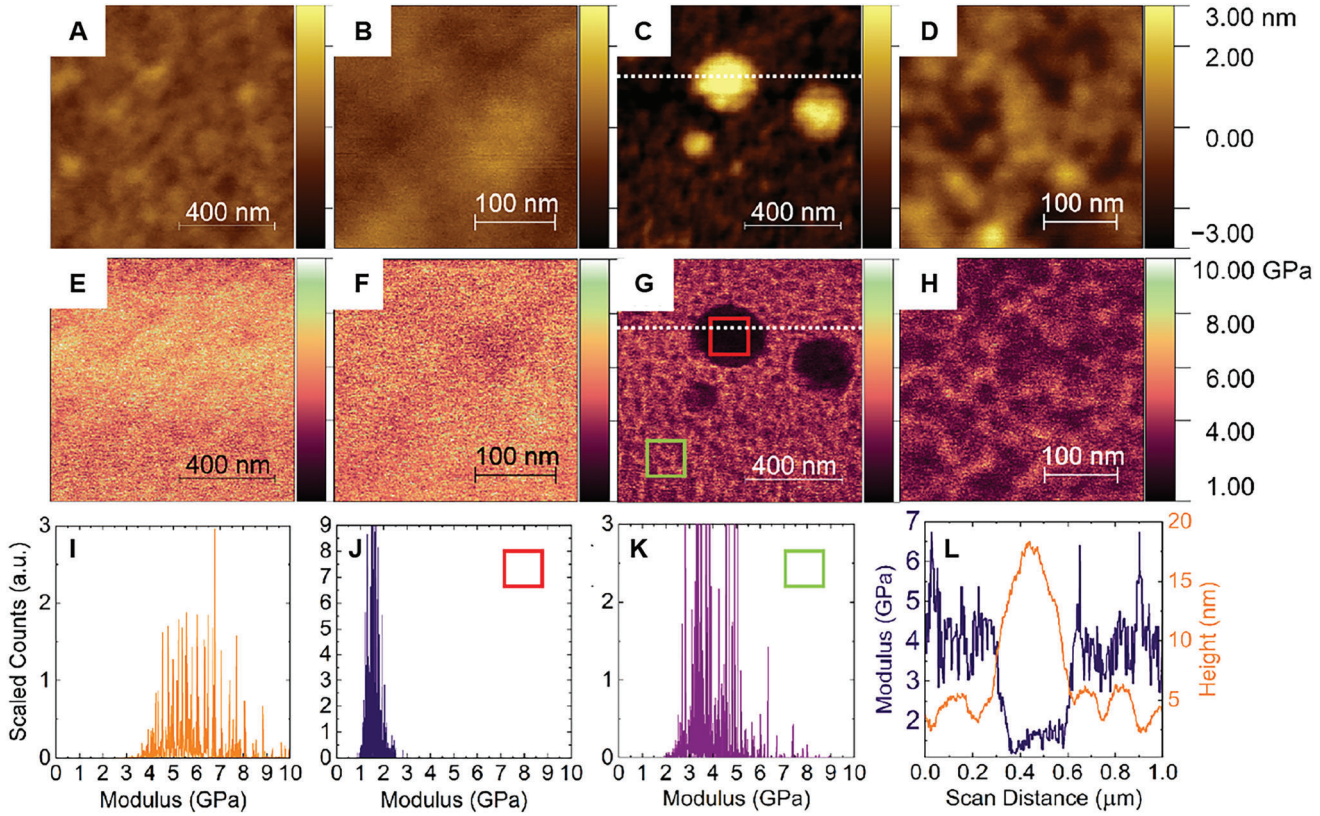

Figure 7. PeakForce QNM topographical scans of 1×1 μm (A,C) and 300×300 nm (B,D) IDTBT films. Clean IDTBT films are depicted in (A,B), and IDTBT films with the PDMS contaminant are depicted in (C,D). The corresponding elastic modulus scans are depicted in (E,F,G,H). The elastic modulus distribution histogram evaluated for the entire area of 1×1 μm clean IDTBT film in (A) is shown in (I). The histogram for the area boxed in red over the PDMS particle is shown in (J), and the histogram for the area boxed in green outside the PDMS particle is shown in (K). The cross-sectional topography and elastic modulus profile along the white dotted lines in (C) and (G) are shown in (L).

wetting behavior of IDTBT films, although the quantities required are larger (i.e., 20 pipettes / 200 μL solution).

In addition to improving wetting behavior, PDMS contamination also improved the performance of IDTBT Cytop-M OFETs, as evidenced by the steeper subthreshold slope of the transfer curves (Figure 6d), as well as an improved and largely gate-voltage independent mobility (Figure 6e). In essence, the "1 needle" sample of Figure 6d was similar to the "0 tips, annealed" sample of Figure 4c. The beneficial effect of the contamination on OFET performance may be due to the improved film uniformity (Figure 6c), and/or due to a similar mechanism as demonstrated previously for small molecule additives intentionally introduced into the films to improve the environmental and electrical stress stability of the devices [see discussion below, Ref. [24]]. However, excessive contamination (5 needles / 200 μL) resulted in reduced mobility, as well as poor wetting by the Cytop-M dielectric (visible in Figure 6c). More diluted Cytop solutions (Cytop to solvent ratio 1:5 v/v) did not dewet from the edges, but still exhibited radial dewetting streaks (Figure S22, Supporting Information). The effect of PDMS contamination on the OFF-state bias stress stability was limited to a slight increase in the threshold voltage (Figure S23, Supporting Information). The molecular weight and/or termination of the PDMS used appears to be important to observe these beneficial effects. Our NMR data suggest that the needles are coated with –Si–$(CH_3)_3$ terminated PDMS, with a molecular weight of ≈360 kDa. Intentionally adding lower molecular weight PDMS, such as standard Sylgard 184 base (≈50 kDa), to the solution did not have the same beneficial effect on the wetting properties. This implies some degree of miscibility between the PDMS and IDTBT is beneficial.

To better visualize the nanoscale interaction between IDTBT and PDMS, we turned to PeakForce Quantitative Nanomechanics (QNM), an atomic force microscope technique that can spatially map the nanomechanical properties of thin films.[65,66] The evaluated elastic moduli should be considered as apparent elastic moduli, due to variation in actual contact area between the end of the tip and surface topography. Nevertheless, the contrast in elastic modulus between different surface areas is clear. We compare clean IDTBT films and films that were made with PDMS-contaminated IDTBT solution (3 needles / 70 μL of solution). Films were prepared in a glovebox that was free of contamination. The topographic and elastic modulus maps of IDTBT thin films, with and without PDMS particles, are shown in **Figure 7**. The films of clean IDTBT are uniform and relatively smooth, as can be concluded from Figure 7a,b showing two different scan areas, at different resolutions. In the PDMS-contaminated films we detect large, presumably PDMS-rich particles that are clearly observable in the topographic images measured at 5 μm × 5 μm (Figure S24,

Table 1. Summary table of contaminants, their origin, effect on devices, and mitigation.

Contaminant	Source	Effect on devices	Mitigation
Volatile and reactive materials (e.g., SAM precursors)	Material off-gassing; sample processing (e.g., SAM fabrication); leaking vials/caps	Irreproducibility; depends on the impurity	Do not store or use volatile chemicals in the glovebox. If infeasible, purge during/after use. Install regenerable solvent trap
Residual solvent	Spin coating, solution preparation, leaking vials/caps	Depends on the solvent	Purge between different solvents. Purge before and during annealing. Install regenerable solvent trap.
Oleamide, monoglycerides	Plastic syringes, plastic micropipettes	Degraded device performance, bias stress instability, increased water uptake	Replace with glass syringes/pipettes
PDMS	Disposable siliconized needles	Enhanced wetting and electrical properties	Replace with silicone oil-free stainless steel needles
Oil mist	Vacuum pump	Untested	Install foreline trap or oil free vacuum pump. Purge glovebox before use. Turn off vacuum pump at night.

Supporting Information) and at 1 μm × 1 μm (Figure 7c). The areas in between these particles show a more uniform height distribution, similar to the clean IDTBT film. Note that contact angle measurements are unable to distinguish between clean and PDMS-contaminated IDTBT films (Figure S25, Supporting Information).

Nanomechanical mapping gives us additional information to more clearly understand the composition of the PDMS-contaminated films. From the apparent elastic modulus map in Figure 7g, we can clearly identify the observed particles as PDMS, owing to their much softer mechanical response and the significant decrease in apparent elastic modulus. This observation is further verified in the apparent elastic modulus histograms evaluated for the entire area of the clean IDTBT film shown in Figure 7i, the region only containing the PDMS particle (red box of Figure 7g) shown in Figure 7j, and the region outside the PDMS particle (green box of Figure 7g) shown in Figure 7k. The region between the particles, which must be the IDTBT-rich phase, displays a modulus that is intermediate between that of the particle and the clean film. This reduction in the modulus of the IDTBT film in between the PDMS particles implies significant solubility of PDMS within the IDTBT. A cross-sectional profile of the topography and elastic modulus measured across one PDMS particle along the dotted white lines of Figure 7c,g is shown in Figure 7l.

While the values of the apparent elastic modulus obtained from the QNM measurements cannot be interpreted directly in terms of literature values of pure PDMS (Figure S24, Supporting Information), due to possible substrate effects and high cantilever stiffness not optimal for such soft materials, the topographical map of Figure 7d and the modulus map of Figure 7h provide evidence for significant miscibility between IDTBT and PDMS. Nanoscale variations in modulus are observed in the IDTBT-rich phase of the PDMS-contaminated films (Figure 7h), in contrast with the quite homogenous modulus observed in the clean film (Figure 7f). The nanoscale miscibility of these two polymers, not apparent from topographic imaging alone, rationalizes the strong effect of the PDMS on wetting behavior and device performance (Figure 6), and demonstrates the utility of nanomechanical measurements.

3. Conclusion

In this study, we investigated the effects of processing-induced contamination on the fabrication and performance of organic electronic devices. **Table 1** summarizes the different contaminants, their origin, their effect on devices, and mitigation. We demonstrated that even small amounts of contaminants can affect the thin-film processing behavior and the electrical properties of devices. These effects were observed in different polymer and small molecule semiconductors. We showed that NMR can be used to detect and quantify contaminants in solutions and thin films, and be used to monitor contamination levels in a glovebox system.

The contaminants were found to originate from both the glovebox atmosphere, as well as laboratory consumables commonly used during film processing (disposable needles, plastic pipettes, and plastic syringes). Accumulated contamination leaching from plastic pipettes leads to degraded device performance and increases the water uptake of polymer films. This water can then lead to a range of effects, including trap formation and reduced mobility, threshold voltage shifts, degraded bias stress stability, and reduced doped film conductivity. Contamination from plastics also affects the morphology and wetting properties of polymer films, the solubility of solid-state additives, as well as the crystallization of small molecule films. Polydimethylsiloxane (PDMS) contamination from siliconized steel needles can enhance the wetting and electrical properties of polymer OFETs.

We also demonstrated that fabricating in a solvent-saturated glovebox atmosphere results in altered device performance, due to residual solvent left in the film, and that this needs to be considered when interpreting the effectiveness of intentionally incorporated molecular additives. The glovebox atmosphere was shown to have a much larger effect on the film's residual solvent content than the annealing conditions. We found it important to adopt rigorous glovebox maintenance and fabrication protocols and to

ensure a clean glovebox processing atmosphere with minimum contamination levels, to ensure reproducibility of film processing conditions and to correctly interpret differences in device performance due to intentional variations in materials composition or device structure.

An in-depth understanding of the sources of contamination during organic electronic device fabrication has allowed us to establish clean fabrication protocols, and make contamination-free samples with improved performance and stability. We recommend that researchers in the field report details of the glovebox solvent trap and purging protocols, and phase out the use of plastic labware, such as micropipettes and syringes. It is important to re-emphasize that the experimental infrastructure and procedures used in our study are similar to those used by many groups in the field for preparing solution-processed organic semiconductor thin films. This suggests that our findings will be helpful to the community, both in re-interpreting some poorly understood literature results, and in establishing clean fabrication protocols for future studies. Furthermore, although our study is focused on OFETs, we believe that the insights gained into the effects of contamination will also be applicable to other device applications that incorporate solution-processed organic semiconductors, such as solar cells and light-emitting diodes.

Supporting Information

Supporting Information is available from the Wiley Online Library or from the author.

Acknowledgements

D.S. and I.E.J. contributed equally to this work. The authors acknowledge funding from the Engineering and Physical Sciences Research Council (EPSRC) (EP/R031894/1, EP/R032025/1, EP/W017091/1). D.S. acknowledges support from the EPSRC Centre for Doctoral Training (CDT) in Sensor Technologies and Applications (EP/L015889/1). I.E.J. acknowledges funding from a Royal Society Newton International Fellowship. A.S. and R.M.O. acknowledge funding from the European Union's Horizon 2020 research and innovation program under the Marie Skłodowska-Curie grant, MultiStem (No. 895801). D.V. acknowledges the Royal Society for funding in the form of a Royal Society University Research Fellowship (Royal Society Reference No. URF\R1\201590). M.G. and H.S. acknowledge funding from the European Union's Horizon 2020 research and innovation program under the Marie Skłodowska-Curie grant agreement, UHMob (No 811284). G.S. thanks the Belgian National Fund for Scientific Research (FNRS) for financial support through research project COHERENCE2 No. F.4536.23. G.S. is an FNRS Research Associate. G.S. acknowledges financial support from the Francqui Foundation (Francqui Start-Up Grant). I.B.D. acknowledges support from the EPSRC Cambridge NanoDTC (EP/L015978/1). H.S. acknowledges funding from a Royal Society Research Professorship (RP\R1\201082). The authors acknowledge support from the Henry Royce Institute facilities grant (EP/P024947/1), as well as the Sir Henry Royce Institute recurrent grant (EP/R00661X/1) for the use of the ambient cluster tool and the EQCM.

Conflict of Interest

H.S. is the Chief Scientist of FlexEnable Ltd.

Data Availability Statement

The data that support the findings of this study are available online, from the Apollo repository (DOI: 10.17863/CAM.99879).[67]

Keywords

contaminants, glovebox systems, organic electronics, pipettes, silicones, syringes, water uptake

Received: April 10, 2023
Revised: June 28, 2023
Published online:

[1] Y.-J. Liu, D. M. Waugh, H.-Z. Yu, *Appl. Phys. Lett.* **2002**, *81*, 4967.
[2] M. Tamaoki, K. Nishiki, A. Shimazaki, Y. Sasaki, S. Yanagi, in *Proceedings of SEMI Advanced Semiconductor Manufacturing Conference and Workshop*, IEEE, Cambridge, MA, USA **1995**, pp. 322–326.
[3] A. Laikhtman, I. Gouzman, R. Verker, E. Grossman, *J. Spacer. Rockets* **2009**, *46*, 236.
[4] F. Sugimoto, S. Okamura, *J. Electrochem. Soc.* **1999**, *146*, 2725.
[5] A. Kahn, *Mater. Horiz.* **2016**, *3*, 7.
[6] J. Drechsel, A. Petrich, M. Koch, S. Pfützner, R. Meerheim, S. Scholz, J. Drechsel, K. Walzer, M. Pfeiffer, K. Leo, *Dig. Tech. Pap. - Soc. Inf. Disp. Int. Symp.* **2006**, *37*, 1692.
[7] C. Yumusak, N. S. Sariciftci, M. Irimia-Vladu, *Mater. Chem. Front.* **2020**, *4*, 3678.
[8] L. I. Leshanskaya, N. N. Dremova, S. Y. Luchkin, I. S. Zhidkov, S. O. Cholakh, E. Z. Kurmaev, K. J. Stevenson, P. A. Troshin, *Thin Solid Films* **2018**, *649*, 7.
[9] M. P. Nikiforov, B. Lai, W. Chen, S. Chen, R. D. Schaller, J. Strzalka, J. Maser, S. B. Darling, *Energy Environ. Sci.* **2013**, *6*, 1513.
[10] S. Griggs, A. Marks, D. Meli, G. Rebetez, O. Bardagot, B. D. Paulsen, H. Chen, K. Weaver, M. I. Nugraha, E. A. Schafer, J. Tropp, C. M. Aitchison, T. D. Anthopoulos, N. Banerji, J. Rivnay, I. McCulloch, *Nat. Commun.* **2022**, *13*, 7964.
[11] H. Klauk, *Organic Electronics: Materials, Manufacturing, and Applications*, Wiley, New York **2006**.
[12] T. W. Lee, S. Tumanov, S. G. Villas-Bôas, J. M. Montgomery, N. P. Birch, *J. Neurochem.* **2015**, *133*, 53.
[13] L. S. Jones, A. Kaufmann, C. R. Middaugh, *J. Pharm. Sci.* **2005**, *94*, 918.
[14] E. Krayukhina, K. Tsumoto, S. Uchiyama, K. Fukui, *J. Pharm. Sci.* **2015**, *104*, 527.
[15] R. Thirumangalathu, S. Krishnan, M. S. Ricci, D. N. Brems, T. W. Randolph, J. F. Carpenter, *J. Pharm. Sci.* **2009**, *98*, 3167.
[16] P. Basu, Sampathkumarkrishnan, R. T., T. W. Randolph, J. F. Carpenter, *J. Pharm. Sci.* **2013**, *102*, 852.
[17] M. Shah, Z. Rattray, K. Day, S. Uddin, R. Curtis, C. F. van der Walle, A. Pluen, *Int. J. Pharm.* **2017**, *519*, 58.
[18] G. R. McDonald, A. L. Hudson, S. M. J. Dunn, H. You, G. B. Baker, R. M. Whittal, J. W. Martin, A. Jha, D. E. Edmondson, A. Holt, *Science* **2008**, *322*, 917.
[19] U. Jug, K. Naumoska, V. Metličar, A. Schink, D. Makuc, I. Vovk, J. Plavec, K. Lucas, *Sci. Rep.* **2020**, *10*, 2163.
[20] A. Olivieri, O. S. Degenhardt, G. R. McDonald, D. Narang, I. M. Paulsen, J. L. Kozuska, A. Holt, *Can. J. Physiol. Pharmacol.* **2012**, *90*, 697.
[21] F. C. Magne, R. R. Mod, E. L. Skau, *J. Am. Oil Chem. Soc.* **1967**, *44*, 235.
[22] J. Mun, J. Kang, Y. Zheng, S. Luo, Y. Wu, H. Gong, J.-C. Lai, H.-C. Wu, G. Xue, J. B.-H. Tok, Z. Bao, *Adv. Electron. Mater.* **2020**, *6*, 2000251.
[23] M. Kang, J.-S. Yeo, W.-T. Park, N.-K. Kim, D.-H. Lim, H. Hwang, K.-J. Baeg, Y.-Y. Noh, D.-Y. Kim, *Adv. Funct. Mater.* **2016**, *26*, 8527.
[24] M. Nikolka, I. Nasrallah, B. Rose, M. K. Ravva, K. Broch, A. Sadhanala, D. Harkin, J. Charmet, M. Hurhangee, A. Brown, S. Illig, P. Too,

J. Jongman, I. McCulloch, J.-L. Bredas, H. Sirringhaus, *Nat. Mater.* **2017**, *16*, 356.
[25] J. K. Sears, J. R. Darby, *The Technology of Plasticizers*, Wiley, New York **1982**.
[26] L. Chang, I. E. Jacobs, M. P. Augustine, A. J. Moulé, *Org. Electron.* **2013**, *14*, 2431.
[27] I. E. Jacobs, F. Wang, Z. I. Bedolla Valdez, A. N. Ayala Oviedo, D. J. Bilsky, A. J. Moulé, *J. Mater. Chem. C* **2018**, *6*, 219.
[28] W. Zhang, J. Smith, S. E. Watkins, R. Gysel, M. McGehee, A. Salleo, J. Kirkpatrick, S. Ashraf, T. Anthopoulos, M. Heeney, I. McCulloch, *J. Am. Chem. Soc.* **2010**, *132*, 11437.
[29] I. McCulloch, R. S. Ashraf, L. Biniek, H. Bronstein, C. Combe, J. E. Donaghey, D. I. James, C. B. Nielsen, B. C. Schroeder, W. Zhang, *Acc. Chem. Res.* **2012**, *45*, 714.
[30] D. Venkateshvaran, M. Nikolka, A. Sadhanala, V. Lemaur, M. Zelazny, M. Kepa, M. Hurhangee, A. J. Kronemeijer, V. Pecunia, I. Nasrallah, I. Romanov, K. Broch, I. McCulloch, D. Emin, Y. Olivier, J. Cornil, D. Beljonne, H. Sirringhaus, *Nature* **2014**, *515*, 384.
[31] H. Bronstein, D. S. Leem, R. Hamilton, P. Woebkenberg, S. King, W. Zhang, R. S. Ashraf, M. Heeney, T. D. Anthopoulos, J. de Mello, I. McCulloch, *Macromol.* **2011**, *44*, 6649.
[32] I. McCulloch, M. Heeney, C. Bailey, K. Genevicius, I. MacDonald, M. Shkunov, D. Sparrowe, S. Tierney, R. Wagner, W. Zhang, M. L. Chabinyc, R. J. Kline, M. D. McGehee, M. F. Toney, *Nat. Mater.* **2006**, *5*, 328.
[33] S. Schott, E. Gann, L. Thomsen, S.-H. Jung, J.-K. Lee, C. R. McNeill, H. Sirringhaus, *Adv. Mater.* **2015**, *27*, 7356.
[34] H. Yan, Z. Chen, Y. Zheng, C. Newman, J. R. Quinn, F. Dötz, M. Kastler, A. Facchetti, *Nature* **2009**, *457*, 679.
[35] U. Zschieschang, F. Ante, D. Kälblein, T. Yamamoto, K. Takimiya, H. Kuwabara, M. Ikeda, T. Sekitani, T. Someya, J. B.- Nimoth, H. Klauk, *Org. Electron.* **2011**, *12*, 1370.
[36] G. Schweicher, G. D'Avino, M. T. Ruggiero, D. J. Harkin, K. Broch, D. Venkateshvaran, G. Liu, A. Richard, C. Ruzié, J. Armstrong, A. R. Kennedy, K. Shankland, K. Takimiya, Y. H. Geerts, J. A. Zeitler, S. Fratini, H. Sirringhaus, *Adv. Mater.* **2019**, *31*, 1902407.
[37] S. K. Park, C.-C. Kuo, J. E. Anthony, T. N. Jackson, in *IEEE International Electron Devices Meeting, 2005. IEDM Technical Digest.*, IEEE, Washington, DC **2005**, pp. 4-108.
[38] T. F. Molinski, *Nat. Prod. Rep.* **2010**, *27*, 321.
[39] J.-F. Chang, B. Sun, D. W. Breiby, M. M. Nielsen, T. I. Sölling, M. Giles, I. McCulloch, H. Sirringhaus, *Chem. Mater.* **2004**, *16*, 4772.
[40] M. Nikolka, G. Schweicher, J. Armitage, I. Nasrallah, C. Jellett, Z. Guo, M. Hurhangee, A. Sadhanala, I. McCulloch, C. B. Nielsen, H. Sirringhaus, *Adv. Mater.* **2018**, *30*, 1801874.
[41] G. Zuo, M. Linares, T. Upreti, M. Kemerink, *Nat. Mater.* **2019**, *18*, 588.
[42] K. C. Dickey, J. E. Anthony, Y.-L. Loo, *Adv. Mater.* **2006**, *18*, 1721.
[43] J. Vogelsang, J. M. Lupton, *J. Phys. Chem. Lett.* **2012**, *3*, 1503.
[44] C. Sinturel, M. Vayer, M. Morris, M. A. Hillmyer, *Macromol* **2013**, *46*, 5399.
[45] M. Nguyen, U. Kraft, W. L. Tan, I. Dobryden, K. Broch, W. Zhang, H.-I. Un, D. Simatos, D. Venkateshavaran, I. McCulloch, P. M. Claesson, C. R. McNeill, H. Sirringhaus, *Adv. Mater.* **2023**, *35*, 2205377.
[46] *MBraun, Options and Spare Parts for Gloveboxes*, **2017**.
[47] D. Hernández-Monje, L. Giraldo, J. C. Moreno-Piraján, *Front. Environ. Chem.* **2020**, *1*, 11.
[48] C. Y. Kao, B. Lee, L. S. Wielunski, M. Heeney, I. McCulloch, E. Garfunkel, L. C. Feldman, V. Podzorov, *Adv. Funct. Mater.* **2009**, *19*, 1906.
[49] M. Kettner, M. Zhou, J. Brill, P. W. M. Blom, R. T. Weitz, *ACS Appl. Mater. Interfaces* **2018**, *10*, 35449.
[50] P. A. Bobbert, A. Sharma, S. G. J. Mathijssen, M. Kemerink, D. M. de Leeuw, *Adv. Mater.* **2012**, *24*, 1146.
[51] I. E. Jacobs, Y. Lin, Y. Huang, X. Ren, D. Simatos, C. Chen, D. Tjhe, M. Statz, L. Lai, P. A. Finn, W. G. Neal, G. D'Avino, V. Lemaur, S. Fratini, D. Beljonne, J. Strzalka, C. B. Nielsen, S. Barlow, S. R. Marder, I. McCulloch, H. Sirringhaus, *Adv. Mater.* **2021**, *34*, 2102988.
[52] D. Simatos, L. J. Spalek, U. Kraft, M. Nikolka, X. Jiao, C. R. McNeill, D. Venkateshvaran, H. Sirringhaus, *APL Mater.* **2021**, *9*, 041113.
[53] J. Malmstrøm, *J. Pharm. Sci.* **2019**, *108*, 1512.
[54] D. Corning, *Silicones in Pharmaceutical Applications. Part 5: Siliconization of Parenteral Packaging Components* **2008**.
[55] G. B. Melo, N. F. S. da Cruz, L. L. do Monte Agra, G. G. Emerson, L. H. Lima, V. Linkuviene, M. Maia, M. E. Farah, J. F. Carpenter, E. B. Rodrigues, C. Probst, *Acta Ophthalmol* **2021**, *99*, e1366.
[56] F. Felsovalyi, S. Janvier, S. Jouffray, H. Soukiassian, P. Mangiagalli, *J. Pharm. Sci.* **2012**, *101*, 4569.
[57] C. F. Chisholm, A. E. Baker, K. R. Soucie, R. M. Torres, J. F. Carpenter, T. W. Randolph, *J. Pharm. Sci.* **2016**, *105*, 1623.
[58] S. Stadtmüller, *Polym. and Polym. Compos.* **2002**, *10*, 49.
[59] G. Wypych (Ed.), *Handbook of Plasticizers*, Elsevier, Toronto **2017**.
[60] E. H. Immergut, H. F. Mark, in *Plasticization and Plasticizer Processes*, American Chemical Society, Washington **1965**, pp. 1–26.
[61] H. Levine (Ed.), *Amorphous Food and Pharmaceutical Systems*, Royal Society Of Chemistry, Cambridge, UK **2002**.
[62] M. Klähn, R. Krishnan, J. M. Phang, F. C. H. Lim, A. M. van Herk, S. Jana, *Polymer* **2019**, *179*, 121635.
[63] M. G. Abiad, M. T. Carvajal, O. H. Campanella, *Food Eng. Rev.* **2009**, *1*, 105.
[64] M. Xiao, A. Sadhanala, M. Abdi-Jalebi, T. H. Thomas, X. Ren, T. Zhang, H. Chen, R. L. Carey, Q. Wang, S. P. Senanayak, C. Jellett, A. Onwubiko, M. Moser, H. Liao, W. Yue, I. McCulloch, M. Nikolka, H. Sirringhaus, *Adv. Funct. Mater.* **2021**, *31*, 2007359.
[65] B. Pittenger, N. Erina, C. Su, *Quantitative Mechanical Property Mapping at the Nanoscale with PeakForce QNM* **2010**, 12.
[66] V. Panchal, I. Dobryden, U. D. Hangen, D. Simatos, L. J. Spalek, I. E. Jacobs, G. Schweicher, P. M. Claesson, D. Venkateshvaran, *Adv. Electron. Mater.* **2021**, *8*, 2101019.
[67] D. Simatos, I. E. Jacobs, I. Dobryden, M. Nguyen, A. Savva, D. Venkateshvaran, M. Nikolka, J. Charmet, L. J. Spalek, M. Gicevičius, Y. Zhang, G. Schweicher, D. J. Howe, S. Ursel, J. Armitage, I. B. Dimov, U. Kraft, W. Zhang, M. Alsufyani, I. McCulloch, R. M. Owens, P. M. Claesson, T. P. J. Knowles, H. Sirringhaus, Research data supporting "Effects of Processing-Induced Contamination on Organic Electronic Devices". Apollo - University of Cambridge Repository **2023**. https://doi.org/10.17863/CAM.99879

